Journal of Solid Mechanics Vol. 9, No. 1 (2017) pp. 172-185

Numerical Investigation of the Mixed-Mode Stress Intensity Factors in FGMs Considering the Effect of Graded Poisson's Ratio

R. Ghajar [1, *], S. Peyman [1], J. Sheikhi [2], M. Poorjamshidian [3]

[1]Department of Mechanical Engineering, K.N. Toosi University ,Tehran, Iran
[2]Department of Civil Engineering ,Razi University , Kermanshah, Iran
[3]Department of Mechanical Engineering, Kashan University ,Kashan, Iran

Received 9 December 2016; accepted 7 February 2017

ABSTRACT

In this paper, the interface crack of two non-homogenous functionally graded materials is studied. Subsequently, with employing the displacement method for fracture of mixed-mode stress intensity factors, the continuous variation of material properties are calculated. In this investigation, the displacements are derived with employing of the functional graded material programming and analysis of isoparametric finite element; then, with using of displacement fields near crack tip, the mixed-mode stress intensity factors are defined. In this present study, the problems are divided into homogenous and non-homogenous materials categories; and in order to verify the accuracy of results, the analytical and numerical methods are employed. Moreover, the effect of Poisson's ratio variation on mixed-mode stress intensity factors for interface crack be examined and is shown in this study. Unlike the homogenous material, the effect of Poisson's ratio variations on mixed-mode stress intensity factors at interface crack between two nonhomogenous is considerable.

Keywords : Interface crack; Displacement method; Nonhomogeneous materials.

1 INTRODUCTION

IN recent years, composite materials have been applied in more and more fields. The interfaces between the components often debond for their poor toughness and hence, the interfacial fracture becomes a key failure mode for these composite materials. The theoretical foundation for interfacial fracture mechanics was laid by Williams [1] due to his rigorous solution of the elastic interface crack problem and the derivation of the characteristic oscillating stress singularity. Then, England [2], Erdogan [3] and Rice and Sih [4] developed the interfacial fracture mechanics by solving some specific problems. Rice [5] gave the complete form of stress and displacement fields in the vicinity of the interface crack tip and offered the interpretation of the complex stress intensity factor (SIF). A complex SIF K with real and imaginary parts K_1 and K_2 implies that tensile and shear effects near the crack tip are intrinsically inseparable. The complete solution to a semi-infinite interface crack between two infinite isotropic elastic layers under edge loading conditions was given by Suo and Hutchinson [6]. A systemic illustration of the previous analytical and experimental works on the interface crack in layered materials was given by Hutchinson and Suo [7].

Among the available numerical methods for determining the parameters characterizing crack-tip fields, J-integral Rice [8] has obtained a great success for its path-independence in homogeneous materials. Smelser and Gurtin [9]

*Corresponding author.
E-mail address: Ghajar@kntu.ac.ir (R. Ghajar).

extended the standard *J*-integral to the interface crack with no change and it was proved to be still path-independent. However, they pointed out that the extension of the J-integral is not valid when the biomaterial interface is not straight. The interaction integral method was combined with the extended finite element method (XFEM) to calculate the mixed-mode SIFs more efficiently for biomaterial interface cracks by Nagashima et al. [10] and Sukumar et al. [11]. The interaction integral can also be employed together with the boundary element method (BEM) to analyze the problems of two-dimensional interface cracks Matsumto et al. [12] or three-dimensional interface cracks Cisilino and Ortiz [13], Ortiz and Cisilino [14] and Johnson and Qu [15] solved the SIFs of three-dimensional curved cracks on a bimaterial interface under nonuniform temperature conditions by the interaction integral technique. Merzbacher and Horst [16] extended the interaction integral to extract the SIFs of interface cracks in layered orthotropic solids.

Most of the previous work was focused on the interface cracks between two homogeneous materials. Meanwhile, for a crack in a continuous body with nonhomogeneous material properties, there is a large quantity of research work on this fracture problem Eischen[17], Erdogan [18], Chen and Erdogan [19], Noda [20], Guler and Erdogan [21] and Guo and Noda [22,23]. Moreover, the interaction integral has been exploited for nonhomogeneous materials for extracting the mixed-mode SIFs and the *T*-stress Dolbow and Gosz [24], Paulino and Kim [25] and Kim and Paulino [26, 27]. Hongjun Yu et al. [28] are employed the interaction integral method to interface crack of two nonhomogeneous materials. In order to calculation of mixed mode stress intensity factors for two nonhomogeneous materials they presented a new form of interaction integral. Due to the lack of analytical fields and numerical solution for the above issue, in order to validation they have been used the comparison of interface crack between two homogeneous materials. This method is needed to appropriate definition of actual and auxiliary fields which is not depend on derivatives of material properties and has its own complexity. However, among the investigations that have been done so far, a small number of related studies are about interface crack between two non-homogenous material, and requires to further examination.

Displacement fields method is also one of the most important directly calculation method for fracture mechanics parameters. This method is employed by Yildirim at al. [29] in order to normal crack on interface of two functionally material under mechanical and thermal loads. Because of its simplicity and lack of special complexity, this method is used to evaluation and calculation of mixed mode stress intensity factors of interface crack between two homogenous and non- homogenous materials, and their accuracy results are compared with other analytical (for interface cracks between two homogeneous materials) and numerical methods. On the other hand, the investigations which have done by Ghajar and Moghaddam [30] show that the effect of Poisson's ratio variation on mixed mode stress intensity factors of penny-shaped is not negligible. Also, the effect of Poisson's ratio on the K_I and K_{II} stress intensity factors has not been done for interface crack of non-homogenous material. Accordingly, the effect of Poisson's ratio variation on mixed mode stress intensity factors is investigated in the present study.

2 INTERFACE FRACTURE MECHANICS

Consider the schematic of a bimaterial interface crack shown in Fig. 1. The crack is located along the interface that is between two semi-infinite planes. Let the plane above the crack be denoted by material 1 with Young's modulus and Poisson's ratio of E_1 and v_1, respectively, and let the plane below the crack be material 2 with corresponding properties of E_1 and v_1. We proceed to summarize some of the essential ingredients of linear elastic interfacial fracture mechanics [5]

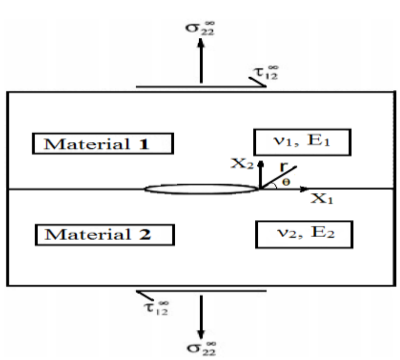

Fig.1
Bimaterial interface crack.

Let $K = K_1 + iK_2$ be the complex stress intensity factor. The in-plane traction vector at a distance r ahead of the crack takes the form [1]

$$\left(\sigma_{22} + i\,\sigma_{12}\right)_{\theta=0} = \frac{K\,r^{i\,\varepsilon^{tip}}}{\sqrt{2\pi r}} \tag{1}$$

where $\mathrm{i} = \sqrt{-1}$, and ε is the bimaterial constant that is defined in Eq. (10). From the above equation, we note that the dimension of K is $[\text{stress}][\text{length}]^{1/2-\mathrm{i}\varepsilon}$, whereas that of its amplitude $|K|$ is the familiar [stress][length]$^{1/2}$. The energy release rate can be related to the stress intensity factor amplitude through the relation [32]

$$\xi = \frac{1}{E^*}\frac{|k|^2}{\cosh(\pi\varepsilon)} \tag{2}$$

$$|k|^2 = k\bar{k} = k_1^2 + k_2^2 \tag{3}$$

$$\frac{2}{E^*} = \frac{1}{\bar{E}_1} + \frac{1}{\bar{E}_2} \tag{4}$$

$$\bar{E} = \begin{cases} E_i & \textit{stress plane} \\ \dfrac{E_i}{1-\nu_i^{\,2}} & \textit{strain plane} \end{cases} \qquad i = (1,2) \tag{5}$$

The phase angle ψ is a measure of the relative proportion of shear to normal tractions at a characteristic distance l ahead of the crack tip. It is defined through the relation [5]

$$kl^{i\varepsilon} = |k|e^{i\psi} \tag{6}$$

$$\psi = tan^{-1}\left(\frac{Im\left[kl^{i\varepsilon}\right]}{Re\left[kl^{i\varepsilon}\right]}\right) \tag{7}$$

The phase angle ψ is an important parameter in the characterization of interfacial fracture toughness. In reporting the phase angle for a given loading configuration, the characteristic length l is taken as the crack (ligament) length or a specimen dimension. It is apparent from the above discussion that, unlike the treatment of cracks in isotropic media, tension and shear effects are inseparable in the vicinity of interface crack tips and as a consequence K_1 and K_2 are not the familiar mode I and mode II stress intensity factors, respectively.

The Cartesian components of the near-tip asymptotic displacement fields can be obtained from Reference [5]. The crack-tip displacement fields in the upper-half plane (replace $\varepsilon\pi$ by $-\varepsilon\pi$ for the lower-half plane) are [33]

$$u_j = \frac{1}{2\mu_1}\sqrt{\frac{r}{2\pi}}\begin{Bmatrix} \mathrm{Re}\left[Kr^{i\varepsilon}\right]\tilde{u}_j^{\,I}\left(\theta,\varepsilon,\vartheta_1\right) + \\ \mathrm{Im}\left[Kr^{i\varepsilon}\right]\tilde{u}_j^{\,II}\left(\theta,\varepsilon,\vartheta_1\right) \end{Bmatrix} \qquad j = (1,2) \tag{8}$$

$$\tilde{u}_1^{I} = A\begin{bmatrix} -e^{2\varepsilon(\pi-\theta)}\left(\cos\frac{\theta}{2}+2\varepsilon\sin\frac{\theta}{2}\right)+ \\ \kappa_1\left(\cos\frac{\theta}{2}-2\varepsilon\sin\frac{\theta}{2}\right)+ \\ \left(1+4\varepsilon^2\right)\sin\frac{\theta}{2}\sin\theta \end{bmatrix} \qquad \tilde{u}_1^{II} = A\begin{bmatrix} e^{2\varepsilon(\pi-\theta)}\left(\sin\frac{\theta}{2}-2\varepsilon\cos\frac{\theta}{2}\right)+ \\ \kappa_1\left(\sin\frac{\theta}{2}+2\varepsilon\cos\frac{\theta}{2}\right)+ \\ \left(1+4\varepsilon^2\right)\cos\frac{\theta}{2}\sin\theta \end{bmatrix}$$

$$\tilde{u}_2^{I} = A\begin{bmatrix} e^{2\varepsilon(\pi-\theta)}\left(\sin\frac{\theta}{2}-2\varepsilon\cos\frac{\theta}{2}\right)+ \\ \kappa_1\left(\sin\frac{\theta}{2}+2\varepsilon\cos\frac{\theta}{2}\right)- \\ \left(1+4\varepsilon^2\right)\cos\frac{\theta}{2}\sin\theta \end{bmatrix} \qquad \tilde{u}_2^{II} = A\begin{bmatrix} e^{2\varepsilon(\pi-\theta)}\left(\cos\frac{\theta}{2}+2\varepsilon\sin\frac{\theta}{2}\right)- \\ \kappa_1\left(\cos\frac{\theta}{2}-2\varepsilon\sin\frac{\theta}{2}\right)+ \\ \left(1+4\varepsilon^2\right)\sin\frac{\theta}{2}\cos\theta \end{bmatrix}$$

where

$$A = \frac{e^{-\varepsilon(\pi-\theta)}}{\left(1+4\varepsilon^2\right)\cosh\left(\pi\varepsilon\right)} \tag{9}$$

and (r,θ) are polar coordinates with origin at the right crack tip. In Eq. (8), Re[·] and Im[·] denote the real and imaginary parts of a complex number, and $r^{i\varepsilon} = e^{i\varepsilon\log r} = \cos(\varepsilon\log r) + i\,\sin(\varepsilon\log r)$. In addition, ε is the bimaterial constant which is a function of β, the second Dundurs parameter [34]:

$$\varepsilon = \frac{1}{2\pi}\log\left(\frac{1-\beta}{1+\beta}\right) \tag{10}$$

$$\beta = \frac{\mu_1\left(k_2-1\right)-\mu_2\left(k_2-1\right)}{\mu_1\left(k_2+1\right)+\mu_2\left(k_1+1\right)} \tag{11}$$

$$k_i = \begin{cases} \dfrac{3-\vartheta_i}{1+\vartheta_i} & \textit{plane stress} \\ 3-4\vartheta_i & \textit{strain plane} \end{cases} \tag{12}$$

where μ_i, ϑ_i and k_i are the shear modulus, Poisson's ratio and the Kolosov constant, respectively, of material i $(i = 1,2)$.

3 INTERACTION INTEGRAL

Interaction integral is one of the methods which are using to calculation of stress intensity factors of homogenous and non-homogenous materials. The base of interaction integral method is according of *J* integral method. The values of *J* integral method for point of b on tip of crack that are shown in Fig. 2 is obtained following equation by using of volume contour which located between A_1, A_2, A_3. At surfaces and crack surfaces of A^+ and A^- [35].

$$J = \int_V \left(\sigma_{ij}u_{i,1} + W\,\delta_{1j}\right)q_{,j}\,dV + \int_V \left(\sigma_{ij}u_{i,1} + W\,\delta_{1j}\right)_{,j} q\,dV \tag{13}$$

while W, v and q represents the strain energy, volume and weigh function respectively, which its value on contour surface is such as:

$$q_k = \begin{cases} l_k, & A_t \\ 0 & A_1, A_2, A_3 \end{cases} \tag{14}$$

The value of q in the middle of the three-dimensional elements, or identical points of Gaussian components are obtained by using of Eq. (15).

$$q_k = \sum_{\alpha=1}^{\alpha=j} N^{\alpha} q_k^{\alpha} \tag{15}$$

α and N^{α} show the nodes of component and their shape function. On the other hand, for linear elasticity material the following relationship is established

$$W = \frac{1}{2}\sigma_{ij}\varepsilon_{ij} \tag{16}$$

By substituting of Eq. (16) in Eq. (13), the J integral for non-homogenous material is rewritten as Eq. (17)

$$J = \int_V \left(\sigma_{ij} u_{i,1} - \frac{1}{2}\sigma_{ik}\varepsilon_{ik}\delta_{1j} \right) q_{,j}\, dV + \int_V \left(\sigma_{ij,j} u_{i,1} + \sigma_{ij} u_{i,1j} - \frac{1}{2}\sigma_{ij,1}\varepsilon_{ij} - \frac{1}{2}\sigma_{ij}\varepsilon_{ij,1} \right) q\, dV \tag{17}$$

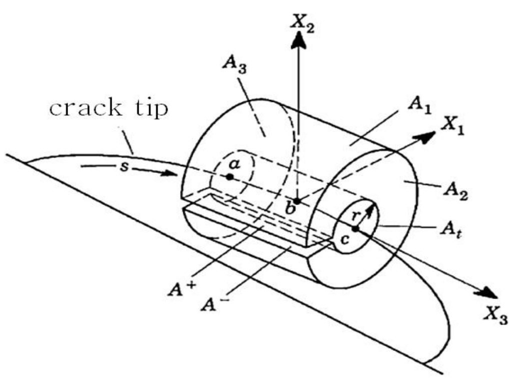

Fig.2
Volume field calculation of interaction integral for definition of stress intensity factors in related of point b on tip of crack.

Eq. (17) is the general form of J integral for functionally material. Based on this equation, J^{aux} integral for auxiliary fields is gained as Eq. (18)

$$J^{aux} = \int_V \left(\sigma_{ij} u_{i,1}^{aux} - \frac{1}{2}\sigma_{\mathrm{ik}}^{aux}\varepsilon_{\mathrm{ik}}^{aux}\delta_{1j} \right) q_{,j}\, dV + \int_V \left(\sigma_{ij,j}^{aux} u_{i,1}^{aux} + \sigma_{ij}^{aux} u_{i,1j}^{aux} - \frac{1}{2}\sigma_{ij,1}^{aux}\varepsilon_{ij}^{aux} - \frac{1}{2}\sigma_{ij}^{aux}\varepsilon_{ij,1}^{aux} \right) q\, dV \tag{18}$$

where

$$\begin{aligned} \sigma_{ij}^{aux} &= \frac{K_I^{aux}}{\sqrt{2\pi r}} f_{ij}^{I}(\theta) + \frac{K_{II}^{aux}}{\sqrt{2\pi r}} f_{ij}^{II}(\theta) + \frac{K_{III}^{aux}}{\sqrt{2\pi r}} f_{ij}^{III}(\theta) \\ u_j^{aux} &= \frac{K_I^{aux}}{2\mu}\sqrt{\frac{r}{2\pi}}\, g_j^{I}(\theta,\nu) + \frac{K_{II}^{aux}}{2\mu}\sqrt{\frac{r}{2\pi}}\, g_j^{II}(\theta,\nu) + \frac{K_{III}^{aux}}{2\mu}\sqrt{\frac{r}{2\pi}}\, g_j^{III}(\theta,\nu) \\ \varepsilon_{ij}^{aux} &= \frac{1}{2}\left(u_{i,j}^{aux} + u_{j,i}^{aux} \right) \end{aligned} \tag{19}$$

Of the real fields $u_i, \sigma_{ij}, \varepsilon_{ij}$ and auxiliary fields $u^{aux}, \sigma^{aux}_{ij}, \varepsilon^{aux}_{ij}$ in Eq. (17), the J^s equation is obtained

$$J^s = \int_V \left(\sigma_{ij} + \sigma^{aux}_{ij}\right)\left(u_{i,1} + u^{aux}_{i,1}\right) q_{,j}\, dV - \frac{1}{2}\int_V \left(\sigma_{ik} + \sigma^{aux}_{ik}\right)\left(\varepsilon_{ik} + \varepsilon^{aux}_{ik}\right)\delta_{1j} q_{,j}\, dV + \int_V \left(\sigma_{ij} + \sigma^{aux}_{ij}\right)\left(u_{i,1} + u^{aux}_{i,1}\right) q dV$$
$$+ \int_V \left(\left(\sigma_{ij,\mathrm{j}} + \sigma^{aux}_{ij,j}\right)\left(u_{i,1j} + u^{aux}_{i,\mathrm{j}}\right)\right) q dV - \frac{1}{2}\int_V \left(\sigma_{ij,1} + \sigma^{aux}_{ij,1}\right)\left(\varepsilon_{ij} + \varepsilon^{aux}_{ij}\right) q dV - \frac{1}{2}\int_V \left(\sigma_{ij} + \sigma^{aux}_{ij}\right)\left(\varepsilon_{ij,1} + \varepsilon^{aux}_{ij,1}\right) q dV \tag{20}$$

Eq. (20) can be considered the sum of three terms as follows:

$$J^s = J + J^{aux} + M \tag{21}$$

In this way, the interaction integral value *M* is represented such as Eq. (22)

$$M = \int_V \left(\sigma_{ij} u_{i,1} + \sigma_{ij} u^{aux}_{i,1}\right) q_{,j} dV - \frac{1}{2}\int_V \left(\sigma_{ik}\varepsilon^{aux}_{ik} + \sigma^{aux}_{ik}\varepsilon_{ik}\right)\delta_{1j} q_{,j} dV + \int_V \left(\sigma_{ij,j} u^{aux}_{i,1} + \sigma^{aux}_{ij,j} u_{i,1} + \sigma_{ij} u^{aux}_{i,1j} + \sigma^{aux}_{ij} u_{i,1j}\right) q dV -$$
$$- \frac{1}{2}\int_V \left(\sigma_{ij}\varepsilon^{aux}_{ij,1} + \sigma^{aux}_{ij}\varepsilon_{ij,1} + \sigma_{ij,1}\varepsilon^{aux}_{ij} + \sigma^{aux}_{ij,1}\varepsilon_{ij}\right) q dV \tag{22}$$

4 BASIC FINITE ELEMENT FORMULATION

Displacements for an isoparametric finite element can be written as:

$$u^e = \sum_{i=1}^{m} N_i u^e_i \tag{23}$$

where N_i are shape functions, u_i is the nodal displacement corresponding to node *i*, and *m* is the number of nodal points in the element. For example, for a *Q*4 element, the standard shape functions are

$$N_i = \left(1 + \xi\xi_i\right)\left(1 + \eta\eta_i\right)/4 \qquad i = 1,\ldots,4 \tag{24}$$

where (ξ, η) denote intrinsic coordinates in the interval [-1,1] and (ξ_i, η_i) denote the local coordinates of node *i*. As usual, strains are obtained from displacements by differentiation as:

$$\varepsilon^e = B^e u^e \tag{25}$$

where $D^e(x)$ is the constitutive matrix, which is a function of position for nonhomogeneous materials, i.e., $D^e(x) = D^e(x, y)$. The principle of virtual work (PVW) yields the following finite element stiffness equations [37]

$$k^e u^e = F^e \tag{26}$$

where F^e is the load vector and the element stiffness matrix is

$$k^e = \int_{\Omega_e} B^{e^T} D^e\left(x\right) B^e\, d\Omega_e \tag{27}$$

In which Ω_e is the domain of element (*e*), and *T* denotes transpose. The reasoning above, at the element level, can be readily extended to the whole domain, which leads to a system of algebraic equations for the unknown displacements [37].

For simplicity of notation, the superscript (*e*), denoting the element, is dropped in this section. Material properties (e.g., at each Gaussian integration point) can be interpolated from the nodal material properties of the element using isoparametric shape functions which are the same for spatial coordinates (x, y) [36]

$$x = \sum_{i=1}^{m} N_i x_i , \; y = \sum_{i=1}^{m} N_i y_i \tag{28}$$

and displacements (u, v)

$$u = \sum_{i=1}^{m} N_i u_i , \; v = \sum_{i=1}^{m} N_i v_i \tag{29}$$

Thus, by generalization of the isoparametric concept, the Young's modulus $E = E(x)$ and Poisson's ratio $\upsilon = \upsilon(x)$ are interpolated as:

$$E = \sum_{i=1}^{m} N_i E_i \; , \; \upsilon = \sum_{i} N_i \upsilon_i \tag{30}$$

The above framework allows development of a fully isoparametric formulation in the sense that the same shape functions are used to interpolate the unknown displacements, the geometry, and the material properties. Thus, the actual variation of the material properties may be approximated by the element interpolation functions (e.g., a certain degree of polynomial functions).

It is clear, functionally elements can approximate the functionally graded material properties better than homogenous elements. Hence, it is essential that employing of isoparametric finite element and functionally element programming for the numerical solving.

5 VERIFICATION AND RESULTS

5.1 Interface crack of two homogenous material

As shown in Fig. 3, an interface crack between two homogeneous elastic semi-infinite planes is considered. The problem with such a configuration was investigated by an analytical approach Rice and Sih [4] and a numerical method Sukumar et al. [11]. According to Sukumar et al. [11], when $W/a \succ 20$, the specimen can be thought to be infinite and hence, W/a is taken to be 30. The exact solution for K_1 and K_2 at the right crack tip was given by Rice [5] as:

$$K = k_1 + ik_2 = \sigma_o \left(1 + 2i\varepsilon\right)\sqrt{\pi a}\left(2a\right)^{-i\varepsilon} \tag{31}$$

The tension load σ_0 is applied along the top and bottom edges of the plate. The displacement boundary conditions are prescribed such that $u_1 = 0$ along the left and right edges and $u_2 = 0$ for the bottom node at the left-hand side. The following data are used for numerical analysis: $W = 30; a = 1; E_1/E_2 = 2 \sim 1000; \upsilon_1 = \upsilon_2 = 0.3; \sigma_0 = 1.0$; generalized plane strain. Eight-node quadrilateral (*Q*8) elements are used over most of the mesh and six-node quarter-point (*T6qp*) singular elements.

The comparison of normalized SIFs computed by Eq.(8) and those given in the references is shown in Table 1. It can be found that the relative errors are all within 5% for K_1/K_0 and 3% for K_2/K_0 compared with exact solution. good agreement indicates that the present method is reliable for interfacial fracture problems.

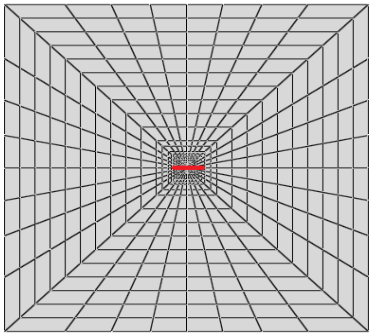

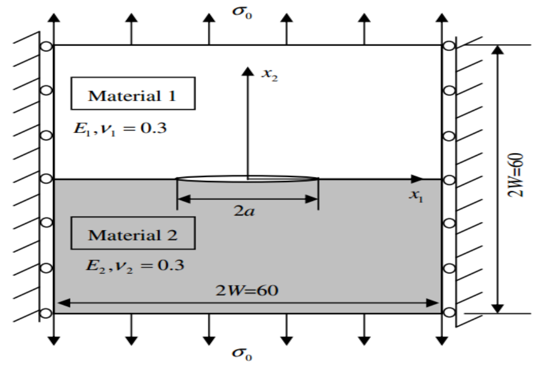

Fig.3
Centered crack between two homogenous plane under tension loading.

Table 1
The values of the first and second modes of stress intensity factors with a centered crack under tension.

E_1/E_2	β	Displacement $w/a=30$		Analytical solving[4] $w/a=30$	
		$k_1(a)/k_0$	$k_2(a)/k_0$	$k_1(a)/k_0$	$k_2(a)/k_0$
2	0.0950	1.010	-0.0406	1.002	-0.0411
4	0.1710	1.022	-0.0770	1.004	-0.0743
8	0.2220	1.051	-0.1000	1.007	-0.0967
20	0.2590	1.055	-0.1119	1.009	-0.1127
40	0.2720	1.056	-0.1198	1.010	-0.1185
100	0.2800	1.059	-0.1212	1.010	-0.1220
1000	0.2850	1.061	-0.1240	1.010	-0.1239

5.2 Interface crack between two nonhomogeneous material plates
5.2.1 Variation of Young's modulus

As shown in Fig. 4, an interface crack between two nonhomogeneous materials is considered. The upper edge of material 1, is under uniform tension loading, equally $\sigma_0 = 1$. The displacement boundary condition for lower edge is $u_2 = 0$, and the lower-left nodal is assumed $u_1 = u_2 = 0$. The Young's modulus for non-homogenous functionally graded material 1 and 2 is such as exponential function that can be expressed as:

$$E_1 = E_0 e^{\delta x_1} \tag{32}$$

$$E_2 = E_0 e^{-\delta x_1} \tag{33}$$

In which, δ is non-homogeneity parameters of functionally graded material that can be formulated as:

$$\delta = \frac{1}{2w} \ln\left(\frac{E_1(w)}{E_1(-w)}\right) \tag{34}$$

The investigated problem for various relation of $E_1(w)/E_1(-w)$ is solved. ϑ_1 and ϑ_2 are the Poisson's ratio of material 1 and 2; respectively, which are shown in Fig. 4. Some numerical details in order to solve this problem are, $E_1 = 1000, E_2 = E_1/10, \sigma_0 = 1, K_0 = \sigma_0\sqrt{\pi a}$ and $\vartheta_1 = \vartheta_2 = 0.3$. In Tables 2. and 3 results are shown for the crack fracture of mixed-mode stress intensity factors, which are compared with displacement and Interaction integral method. It is observed, that achieving answers by this method have good accuracy.

5.2.2 Linear variation of Young's modulus

In this section, the problem of Fig. 4 for the condition that young's modulus in functionally graded material is linear, has been solved. The problem for non-homogenous functionally graded materials in figure as plane stress analytical and Young's modulus, are defined such as:

$$E_1 = E_0\left(\frac{k+1}{2\sqrt{k}} + \frac{k-1}{\sqrt{k}}\frac{x_1}{2w}\right) \tag{35}$$

$$E_2 = E_0\left(\frac{k+1}{2\sqrt{k}} - \frac{k-1}{\sqrt{k}}\frac{x_1}{2w}\right) \tag{36}$$

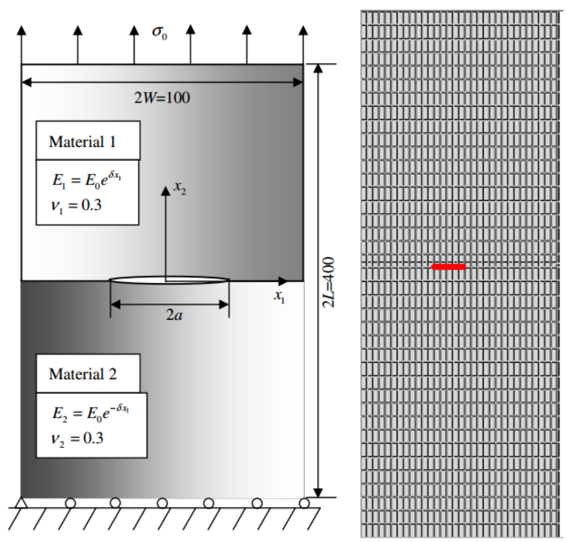

Fig.4
Centered crack between two non-homogenous plane under tension loading.

In which, $k = E_1(w)/E_1(-w)$ is the Young's modulus variation of material. Some significant details of this problem are; $E_1 = 1000, E_2 = E_1/10, \sigma_0 = 1, K_0 = \sigma_0\sqrt{\pi a}$ and $\vartheta_1 = \vartheta_2 = 0.3$. Stress intensity factors for interface crack are presented according of Tables 4. and 5. It is observed, the stress intensify for exponential and linear variation which achieved of isoparametric finite element and displacement method, are so near to analytical results and showing the accuracy of results.

Table 2
Normalized mode-I SIF for interface crack between two exponential non-homogenous materials.

Method	$\frac{E_1(w)}{E_1(-w)}$	$\frac{K_1(a)}{\sigma_0\sqrt{\pi a}}$				
		$a/w=0.2$	$a/w=0.3$	$a/w=0.4$	$a/w=0.5$	$a/w=0.6$
Displacement	1	1.065	1.091	1.101	1.160	1.251
	10	1.252	1.288	1.310	1.389	1.483
	100	1.822	1.837	1.842	1.861	1.880
	1000	2.619	2.581	2.347	2.251	2.199
Interaction Integral[28]	1	1.030	1.061	1.121	1.190	1.310
	10	1.240	1.280	1.330	1.401	1.502
	100	1.820	1.830	1.833	1.842	1.874
	10000	2.591	2.503	2.387	2.210	2.215

Table 3
Normalized mode-II SIF for interface crack between two exponential nonhomogenous materials.

Method	$\frac{E_1(w)}{E_1(-w)}$	$\frac{K_2(a)}{\sigma_0\sqrt{\pi a}}$				
		$a/w = 0.2$	$a/w = 0.3$	$a/w = 0.4$	$a/w = 0.5$	$a/w = 0.6$
Displacement	1	0	0	0	0	0
	10	-0.1123	-0.1200	-0.1213	-0.1220	-0.1230
	100	-0.1775	-0.1901	-0.1941	-0.1949	-0.1953
	1000	-0.2290	-0.2770	-0.2890	-0.2801	-0.2730
Interaction Integral[28]	1	0	0	0	0	0
	10	-0.1115	-0.1210	-0.1200	-0.1190	-0.1190
	100	-0.1700	-0.1880	-0.1930	-0.1910	-0.1932
	10000	-0.2360	-0.2720	-0.2780	-0.2710	-0.2690

Table 4
Normalized mode-I SIF for interface crack between two linear nonhomogenous materials.

Method	$\frac{E_1(w)}{E_1(-w)}$	$\frac{K_1(a)}{\sigma_0\sqrt{\pi a}}$				
		$a/w = 0.2$	$a/w = 0.3$	$a/w = 0.4$	$a/w = 0.5$	$a/w = 0.6$
Displacement	1	1.059	1.084	1.129	1.223	1.338
	10	1.371	1.399	1.471	1.538	1.673
	100	1.539	1.596	1.701	1.811	2.019
Interaction Integral[28]	1	1.030	1.060	1.110	1.190	1.310
	10	1.330	1.370	1.440	1.520	1.650
	100	1.520	1.580	1.670	1.790	1.960

Table 5
Normalized mode-II SIF for interface crack between two linear non-homogenous materials.

Method	$\frac{E_1(w)}{E_1(-w)}$	$\frac{K_2(a)}{\sigma_0\sqrt{\pi a}}$				
		$a/w = 0.2$	$a/w = 0.3$	$a/w = 0.4$	$a/w = 0.5$	$a/w = 0.6$
Displacement	1	0	0	0	0	0
	10	-1.226	-1.292	-1.332	-1.357	-1.444
	100	-1.617	-1.742	-1.823	-1.947	-2.169
Interaction Integral[28]	1	0	0	0	0	0
	10	-1.210	-1.280	-1.310	-1.340	-1.410
	100	-1.600	-1.720	-1.810	-1.920	-2.140

6 EVALUATION EFFECT OF POISSON's RATIO GRADATION ON SIFs

Poisson's ratio is an important factor for fracture of functionally graded materials (FGMs). It may have significant influence on fracture parameters (e.g. stress intensity factors and *T*-stress) for a crack in FGMs under mixed-mode loading conditions, while its effect on such parameters is negligible in homogeneous materials. For instance, when tension load is applied in the direction parallel to material gradation, the fracture parameters may show significant influence on the Poisson's ratio [31]. In this study for various of a/W, the crack fracture of mixed-mode stress intensity factors is calculated; then, the variance percent of constant Poisson's ratio with functionally Poisson's ratio is compared. Hence, the problem of Fig. 4 is studied in this section, again.

$$E_1 = E_0 e^{\delta x_1} \text{ , } E_1 = E_0 e^{-\delta x_1} \tag{37}$$

$$\vartheta_1 = \vartheta_0 e^{\eta x_1}\ ,\ \vartheta_2 = \vartheta_0 e^{-\eta x_1} \tag{38}$$

δ derived by Eq. (34), and η can be written as:

$$\eta = \frac{1}{2w}\ln\left(\frac{\vartheta_1(w)}{\vartheta_1(-w)}\right) \tag{39}$$

It is seen that, difference between mix-mode stress intensify factors for the condition which Poisson's ratio is varied functionally, 5-15 percent is more than the constant Poisson's ratio condition. Now a sensitivity analysis is carried out to demonstrate the trend of K_I and K_{II} with respect to δ and η. These are shown in Tables 8. and 9. For better clarity of the effect of Poisson's ratio gradation on SIFs, the percentage change in SIFs due to change in η for a given δ is also shown in parenthesis in the relevant tables. It is observed that K_I depends on gradation of both modulus of elasticity and Poisson's ratio. On the other hand, it is obvious that the influence of gradation of Poisson's ratio is considerable. For instance for $\delta = 0.023$, difference between K_{IN} for $\eta = 0.002$ and $\eta = 0$ is 13%. Ghajar and Moghaddam [30] by considering of gradation indexes for modulus of elasticity and Poisson's ratio were calculated the mode III stress intensity factors for Penny-shaped crack in a solid cylinder by *J* integral method. It is realized that for a given geometry and boundary condition, K_{III} depends on gradation of both modulus of elasticity and Poisson's ratio.

Table 6
Comparing of the first mode of stress intensity factors for interface crack with exponential and constant of Poisson's ratio variation (the percentage change in K_I due to change Poisson's ratio).

Method	$\frac{E_1(w)}{E_1(-w)}$	$\frac{\upsilon_1(w)}{\upsilon_1(-w)}$	$\frac{K_1(a)}{\sigma_0\sqrt{\pi a}}$				
			$a/w=0.2$	$a/w=0.3$	$a/w=0.4$	$a/w=0.5$	$a/w=0.6$
Displacement	1	1	1.065(0)	1.091 (0)	1.101(0)	1.160(0)	1.251(0.0)
	10	1.25	1.305(4.3)	1.374(6.7)	1.430(9.2)	1.543(11)	1.687(13.8)
	100	1.50	1.956(7.4)	2.013(9.6)	2.050(11.3)	2.11 (13.4)	2.182(16.1)
	1	1	1.065	1.091	1.101	1.160	1.251
	10	1	1.252	1.288	1.310	1.389	1.483
	100	1	1.822	1.837	1.842	1.861	1.880

Table 7
Comparing of the second mode of stress intensity factors for interface crack with exponential and constant of Poisson's ratio variation (the percentage change in K_{II} due to change Poisson's ratio).

Method	$\frac{E_1(w)}{E_1(-w)}$	$\frac{\upsilon_1(w)}{\upsilon_1(-w)}$	$\frac{K_2(a)}{\sigma_0\sqrt{\pi a}}$				
			$a/w=0.2$	$a/w=0.3$	$a/w=0.4$	$a/w=0.5$	$a/w=0.6$
Displacement	1	1	0(0)	0(0)	0(0)	0(0)	0(0.0)
	10	1.25	-0.1166(3.9)	-0.1272(6)	-0.1319(8.8)	-0.1350(10.7)	-0.1384(12.7)
	100	1.50	-0.1888(6.4)	-0.2054(8.1)	-0.2144(10.5)	-0.2204(13.1)	-0.1253(15.4)
	1	1	0	0	0	0	0
	10	1	-0.1123	-0.1200	-0.1213	-0.120	-0.1230
	100	1	-0.1775	-0.1901	-0.1941	-0.1949	-0.1953

Table 8
Sensitivity of K_I to gradation indexes η and δ for interface crack (the percentage change in K_I due to change in η for a given δ is shown in parenthesis).

η	δ					
	0	0.0150	0.0184	0.0205	0.0219	0.0230
0	1.020	1.023	1.035	1.047	1.060	1.781
0.0005	1.021(0.1)	1.035(1.3)	1.051(1.6)	1.068(2.1)	1.093(3.2)	1.850(3.9)
0.0009	1.025(0.5)	1.045(2.2)	1.062(2.7)	1.086(3.8)	1.114(5.1)	1.891(6.2)
0.0013	1.033(1.3)	1.054(3.1)	1.075(3.9)	1.108(5.9)	1.129(6.6)	1.919(7.8)
0.0017	1.037(1.7)	1.066(4.3)	1.095(5.8)	1.122(7.2)	1.142(7.8)	1.941(9.0)
0.0020	1.041(2.1)	1.084(6.0)	1.112 (7.5)	1.141(9.0)	1.176(11.0)	2.011(13.0)

Table 9
Sensitivity of K_{II} to gradation indexes η and δ for interface crack (the percentage change in K_{II} due to change in η for a given δ is shown in parenthesis).

η	δ					
	0	0.0150	0.0184	0.0205	0.0219	0.0230
0	-0.00230	-0.1022	-0.1211	-0.1454	-0.1633	-0.1857
0.0005	-0.002307 (0.3)	-0.1027(0.5)	-0.1218(0.6)	-0.1467(0.9)	-0.1667(2.1)	-0.1907(2.7)
0.0009	-0.002311(0.5)	-0.1033(1.1)	-0.1229(1.5)	-0.1491(2.6)	-0.1696(3.9)	-0.1949(5.0)
0.0013	-0.002316(0.7)	-0.1041(1.9)	-0.1243(2.7)	-0.1522(4.7)	-0.1721(5.4)	-0.1979(6.6)
0.0017	-0.002320(0.9)	-0.1053(3.1)	-0.1266(4.6)	-0.1541(6.0)	-0.1740(6.6)	-0.2001(7.8)
0.0020	-0.002323(1.1)	-0.1064(4.2)	-0.1287(6.3)	-0.1567(7.8)	-0.1793(9.8)	-0.2053(10.6)

7 CONCLUSIONS

In the present work, the modes I and II stress intensity factor in FGMs considering gradation on elastic properties has been numerically investigated. In order to solve the problems, the displacement fields and isoparametric finite element analysis are employed. Because of the complexity of analytical method in interface crack of two non-homogenous material and existence derivatives of material properties and, complexity of problem on tip of crack, this method are presented. To assess the accuracy of the present numerical scheme, benchmark solutions from literature available for homogeneous material and FGMs were studied. It was observed that accurate results are obtained compared to the reference solutions. Further, to investigate the influence of elastic properties on the modes of I and II SIFs, different scale of gradation for both modulus of elasticity and Poisson's ratio were considered. It was observed that generally gradation of modulus of elasticity has more influence on K_I and K_{II}. However its influence is altered for different crack geometries and gradation index. Percentage changes in K_I and K_{II} due to change in η for a given β was drawn in relevant tables for better clarity of the effect of gradation of Poisson's ratio. It was concluded that the influence of gradation of Poisson's ratio can be non-negligible and has to be taken into account, e.g. penny-shaped crack in a solid cylinder and interface crack. Percentage changes in K_I and K_{II} depend on the crack geometry and gradation indexes η and β. Generally, it is inferred that accurate estimation of modes K_I and K_{II} SIFs require a numerical scheme to account for gradation of modulus of elasticity and Poisson's ratio, as well.

REFERENCES

[1] Williams M.L., 1959, The stresses around a fault or crack in dissimilar media, *Bulletin of the Seismological Society of America* **49** (2): 199-204.
[2] England A.H., 1965, A crack between dissimilar media, *Journal of Applied Mechanics* **32**: 400-402.
[3] Erdogan F., 1965, Stress distribution in bonded dissimilar materials with cracks, *Journal of Applied Mechanics* **32**: 403- 410.
[4] Rice J.R., Sih G.C., 1965, Plane problems of cracks in dissimilar media, *Journal of Applied Mechanics* **32**: 418-423.
[5] Rice J.R., 1988, Elastic fracture mechanics concepts for interfacial cracks, *Journal of Applied Mechanics* **55**: 98-103.

[6] Hutchinson J.W., Mear M.E., Rice J.R., 1987, Crack paralleling an interface between dissimilar materials, *Journal of Applied Mechanics* **54**: 828-832.
[7] Hutchinson J.W., Suo Z., 1992, Mixed mode cracking in layered materials, *Advances in Applied Mechanics* **29**: 63-191.
[8] Rice J.R., 1968, A path independent integral and the approximate analysis of strain concentration by notches and cracks, *Journal of Applied Mechanics* **35**: 379-386.
[9] Smelser R.E., Gurtin M.E., 1977, On the *J*-integral for bi-material bodies, *International Journal of Fracture* **13**: 382-384.
[10] Nagashima T., Omoto Y., Tani S., 2003, Stress intensity factor analysis of interface cracks using X-FEM, *International Journal for Numerical Methods in Engineering* **56**: 1151-1173.
[11] Sukumar N., Huang Z.Y., Prévost J.H., Suo Z., 2004, Partition of unity enrichment for bimaterial interface cracks, *International Journal for Numerical Methods in Engineering* **59**: 1075-1102.
[12] Matsumto T., Tanaka M., Obara R., 2000, Computation of stress intensity factors of interface cracks based on interaction energy release rates and BEM sensitivity analysis, *Engineering Fracture Mechanics* **65**: 683-702.
[13] Cisilino A.P., Ortiz J.E., 2005, Three-dimensional boundary element assessment of a fibre/matrix interface crack under transverse loading, *Computers and Structures* **83**: 856-869.
[14] Ortiz J.E., Cisilino A.P., 2005, Boundary element method for *J*-integral and stress intensity factor computations in three-dimensional interface cracks, *International Journal of Fracture* **133**: 197-222.
[15] Johnson J., Qu J.M., 2007, An interaction integral method for computing mixed mode stress intensity factors for curved bimaterial interface cracks in nonuniform temperature fields, *Engineering Fracture Mechanics* **74**: 2282-2291.
[16] Merzbacher M.J., Horst P., 2009, A model for interface cracks in layered orthotropic solids: convergence of modal decomposition using the interaction integral method, *International Journal for Numerical Methods in Engineering* **77**: 1052-1071.
[17] Eischen J.W., 1987, Fracture of nonhomogeneous materials, *International Journal of Fracture* **34**: 3-22.
[18] Erdogan F., 1995, Fracture mechanics of functionally graded materials, *Composites Engineering* **5** (7): 753-770.
[19] Chen Y.F., Erdogan F., 1996, The interface crack problem for a nonhomogeneous coating bonded to a homogeneous substrate, *Journal of the Mechanics and Physics of Solids* **44**: 771-787.
[20] Noda N., 1999, Thermal stresses in functionally graded materials, *Journal of Thermal Stresses* **22** (4-5):477-512.
[21] Guler M.A., Erdogan F., 2006, Contact mechanics of two deformable elastic solids with graded coatings, *Mechanics of Materials* **38** (7): 633-647.
[22] Guo L.C., Noda N., 2007, Modeling method for a crack problem of functionally graded materials with arbitrary properties – piece wise exponential model, *International Journal of Solids and Structures* **44**(21): 6768-6790.
[23] Guo L.C., Noda N., 2008, Fracture mechanics analysis of functionally graded layered structures with a crack crossing the interface, *Mechanics of Materials* **40** (3):81-99.
[24] Dolbow J.E., Gosz M., 2002, On the computation of mixed-mode stress intensity factors in functionally graded materials, *International Journal of Solids and Structures* **39**: 2557-2574.
[25] Paulino G.H., Kim J.H., 2004, A new approach to compute *T*-stress in functionally graded materials by means of the interaction integral method, *Engineering Fracture Mechanics* **71**: 1907-1950.
[26] Kim J.H., Paulino G.H., 2003, *T*-stress, mixed-mode stress intensity factors, and crack initiation angles in functionally graded materials: a unified approach using the interaction integral method, *Computer Methods in Applied Mechanics and Engineering* **192**: 1463-1494.
[27] Kim J.H., Paulino G.H., 2005, Consistent formulations of the interaction integral method for fracture of functionally graded materials, *Journal of Applied Mechanics* **72**: 351-364.
[28] Hongjun Yu., Linzhi Wu ., Licheng Guo., Qilin He., Shanyi Du., 2009, Interaction integral method for the interfacial fracture problems of two nonhomogeneous materials, *Journal of Applied Mechanics of Materials* **42**: 435 -450.
[29] Yildrim B., Dag S., Erdogan F., 2005, Three dimensional fracture analysis of FGM coatings under thermomechanical loading, *International Journal of Fracture* **132**: 369-395.
[30] Ghajar R., Moghaddam A.S., 2010, Numerical investigation of the mode III stress intensity factors in FGMs consideringthe effect of graded Poisson's ratio, *Engineering Fracture Mechanics* **78**: 1478-1486.
[31] Paulino G.H., Kim J.H., 2004, On the poisson's ratio effect on mixed-mode stress intensity factors and T-stress in functionally graded materials, *International Journal of Computational Engineering Science* **5**: 833-861.
[32] Malyshev B.M., Salganik R.L., 1965, The strength of adhesive joints using the theory of cracks, *International Journal of Fracture* **1**: 114-128.
[33] Suo Z., 1989, *Mechanics of Interface Fracture*, Ph.D. Thesis, Division of Applied Sciences, Harvard University, Cambridge, MA, U.S.A.

[34] Dundurs J., 1969, Edge-bonded dissimilar orthogonal elastic wedges, *Journal of Applied Mechanics* **36**: 650-652.

[35] Walters M. C., Paulino G. H., Dodds R. H., 2006, Computation of mixed-mode stress intensity factors for cracks in three-dimensional functionally graded solids, *Journal of Engineering Mechanics* **132**: 1-15.

[36] Kim J.H., Paulino G.H.,2002, Isoparametric graded finite elements for nonhomogeneous isotropic and orthotropic materials, *Journal of Applied Mechanics* **69**: 502-514.

[37] Hughes T. J. R., 1987, *The Finite Element Method: Linear Static and Dynamic Finite Element Analysis*, Prentice-Hall, Englewood Cliffs, NJ.